ACS Catalysis

Research Article

pubs.acs.org/acscatalysis

Effect of Reaction Conditions on the Direct Synthesis of Hydrogen Peroxide with a AuPd/TiO_2 Catalyst in a Flow Reactor

Simon J. Freakley, Marco Piccinini, Jennifer K. Edwards, Edwin N. Ntainjua, Jacob A. Moulijn, and Graham J. Hutchings*

Cardiff University, School of Chemistry, Main Building, Park Place, Cardiff, CF10 3AT, United Kingdom

Supporting Information

ABSTRACT: The direct synthesis of hydrogen peroxide (H_2O_2) represents a potential alternative to the currently industrially used anthraquinone process, and Au−Pd catalysts have been identified as effective catalysts. To obtain a direct process, a detailed understanding of the reaction conditions in a continuous flow system is needed. In this study, we use a flow reactor to study reaction conditions independently, including total gas flow rate, catalyst mass, reaction pressure, solvent flow rate, and H_2/O_2 molar ratio. The study was carried out without the addition of any halide or acid additives often used to suppress the sequential hydrogenation and decomposition reactions that allowed the kinetics of these reactions to be studied along with the synthesis reaction. A global kinetic model describing the net and gross synthesis rate is proposed, and on the basis of this model, we propose that the decomposition reaction suppresses the production of H_2O_2 to a greater extent than hydrogenation and that catalyst design studies should aim at blocking or generating catalysts without O−O dissociation sites.

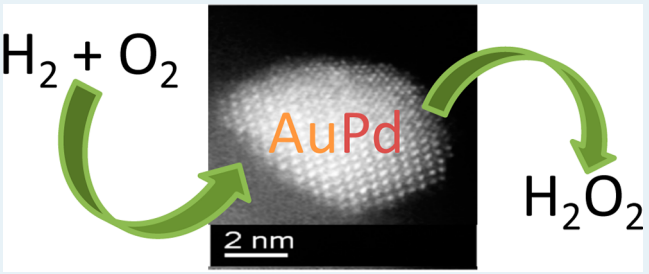

KEYWORDS: *hydrogen peroxide, flow reactor, kinetics, gold, palladium catalyst*

INTRODUCTION

The direct synthesis of hydrogen peroxide (H_2O_2) from molecular H_2 and O_2 represents an attractive alternative to the current large-scale anthraquinone process. Although the current industrial process is viable at a large scale, the production and transportation of concentrated (50−75 wt %) H_2O_2 increases the risk of accidents when the typical end use requires only concentrations of 3−5 wt %. The direct synthesis of H_2O_2 would provide an atom-efficient, on-site way of producing H_2O_2 and avoid the need to transport H_2O_2 in a concentrated form.

Although the direct synthesis from H_2 and O_2 seems to be a viable candidate to produce H_2O_2 industrially, most of the catalysts active for H_2O_2 synthesis are also active for its subsequent decomposition/hydrogenation reactions, leading to low H_2 selectivities.[1] Supported monometallic Pd[2−10] and bimetallic Au−Pd[11−22] catalysts have been extensively investigated for this direct process. Although the monometallic Pd catalysts are the most widely studied, Au−Pd bimetallic catalysts have been shown to be significantly more effective in experimental[11−22] and by computational studies.[23] Moreover, the use of these more active Au−Pd catalysts eliminates the need for the addition of acid and halide additives that are typically added to the reaction medium to enhance the performance of conventional monometallic Pd catalysts. The addition of acid and halide to the reaction medium is undesirable for industrial purposes because this leads to corrosion of reaction vessels in addition to an increase in process cost due to subsequent separation of additives from the product.

A number of different approaches to a direct synthesis process have been investigated. It is crucial to limit the contact between high-pressure H_2 and O_2 during a direct process, either by separating the gases or operating outside the explosive regime. The application of permeable membrane reactors allows the use of concentrated H_2 and O_2 and can achieve H_2O_2 concentrations of 1−10%.[24−28] The membranes of these reactors are coated with AuPd or Pd nanoparticles; however, the application of these types of reactors is limited by the fact that acid/halide promoters are required to achieve high H_2 selectivity and H_2O_2 concentrations. The main challenge in developing membrane reactor configurations is the synthesis of a robust membrane exhibiting satisfactory diffusion rates of hydrogen. For comparison, hydrogen peroxide production rates measured in different reactor systems are shown in Table 1.

Another type of reactor that has been developed to study the direct synthesis process using gas compositions in the explosive regime is microreactors,[29−35] which have internal channels around 1 mm in diameter where effective packing of the catalysts prevents reactions that could lead to an explosion. The recent literature shows promising results in terms of productivity,[34,35] and for comparison, the data are shown in

Received: September 26, 2012
Revised: January 28, 2013
Published: February 6, 2013

Table 1

reference	reactor system	catalyst	temp, K	pressure, Bar	solvent	productivity, mol/kg(Pd)/h
Pashkova[26]	membrane	Pd	293	67	MeOH + H_2O + acid + NaBr	1960
Pashkova[27]	membrane	Pd/TiO_2	293	50	MeOH + acid + NaBr	up to 1700
Weynbergh[10]	batch	5% Pd/Al_2O_3	293	80	1.6 M phosphoric acid + NaBr	16400
Paskova[26]	semibatch	5% Pd/Al_2O_3	293	70	MeOH	6500
Edwards[15]	batch	2.5% Au/2.5% Pd/carbon (acid washed)	275	40	MeOH + H_2O	6400
Inoue[35]	microreactor; particle size ∼ 50 μm	5% Pd/Al_2O_3	293	9.5	acid + NaBr	up to 3000
Inoue[34]	microreactor	5% Pd/various	293	10	H_2O + acid + Br	900
Kim[40]	upflow fixed bed	0.24% Pd/resin	295	50	MeOH + HBr	5290
Biasi[38]	trickle bed reactor particle size −0.5 to 1 mm	2.5% Pd/CeO_2, ZrO_2	263	10	MeOH	40−50
Biasi[39]	trickle bed reactor	2.5% $AuPd/CeO_2$, ZrO_2	263	10	MeOH	up to 180
present paper	microreactor; particle size −200 to 500 μm	1% Au−Pd/TiO_2	275	10	66% MeOH + 34% H_2O	400

Table 1. Microreactors show a possible avenue to develop small-scale, on-site H_2O_2 generation; however, the safety of using explosive gas mixtures on-site has to be taken into account. Using a microreactor packed with Pd catalysts, Volshin[31−33] studied the kinetics of the synthesis and the competing hydrogenation and decomposition reactions and showed that the formation of hydrogen peroxide followed a Langmuir−Hinshelwood mechanism over a supported Pd catalyst. They also demonstrated the dramatic effect of reaction conditions, including temperature, pressure, and pH_2, have on the H_2O_2 selectivity and H_2 conversion using a Pd catalyst. Their results are corroborated by groups carrying out kinetic studies in batch reactors using both supported Pd catalysts[36] and Pd-PVP solutions[37] in the presence of Br^- ions.

Small-scale, fixed-bed reactors operating outside the explosive O_2/H_2 regime have been employed in continuous[38,39] modes of operation. Biasi et al. have shown that it is important to tailor the reaction conditions to the catalyst employed (AuPd or Pd) to achieve high H_2O_2 synthesis rates. Conditions such as gas flow rate, gas composition, and solvent flow rate control the rate of synthesis and affect selectivity toward H_2O_2 just as the choice of catalyst can, and the conditions which provide the highest rate with one catalyst may not necessarily be the best for all catalysts. Typical H_2 selectivities reported are 60−70%. Kim et al.[40] have approached the problem by immobilizing Pd on functionalized resins and shown that these can also be used in a continuous system to produce H_2O_2 with good productivity (Table 1). Absolute comparisons of reaction rates and selectivity between research groups is, in fact, very difficult because of the many various conditions used in all these studies, including catalyst formulation, reactor type, and reaction conditions, including the addition of stabilizers to the reaction mixture.

To provide a commercial alternative to the current anthraquinone process, H_2O_2 concentrations of 6−8 wt % and high H_2 selectivities (>95%) must be achieved with a stable catalyst in the absence of acid or halide promoters, with a simple fixed-bed, continuous process being highly desirable for industrial purposes.

The aim of the study is to investigate the use of a multiphase flow system to study the reaction parameters for the direct synthesis of H_2O_2 under flow conditions. This study will look at the use of a supported Au−Pd catalyst to produce H_2O_2 in the absence of acid and halide promoters. The catalyst we have chosen to study is a Au−Pd catalyst prepared by an excess anion methodology that we have recently reported.[41] This catalyst preparation method produces catalysts that contain only homogeneous bimetallic alloys of Au−Pd, in which all the particles are of the same composition and have a very tight particle size distribution.

The conditions investigated include gas flow rate, pressure, temperature, H_2/O_2, solvent composition, and solvent flow rate. Also included in this study is an investigation into whether the synthesis, decomposition, and hydrogenation rate data can be extracted to give global kinetic information. The use of a catalyst with a tight particle size and composition distribution will allow the study of the kinetics of the process over very specific nanoparticles without having to be concerned with the deconvolutions of the reaction rates of large and small particles of varying composition. The reaction scheme for the synthesis of H_2O_2, including its subsequent hydrogenation and decomposition, is shown in Scheme 1.

Scheme 1. Reaction Scheme of the Direct Synthesis of H_2O_2.

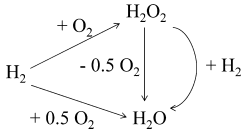

It has been previously postulated,[20] that all of the reactions involved in the direct synthesis of H_2O_2 share the same intermediate reaction species and that H_2O_2 is formed by a 2-step hydrogenation of adsorbed O_2. The key reaction steps for the synthesis of H_2O_2 are shown in Schemes 2 and 3, where * denotes a vacant site on the catalyst surface,

Scheme 2. Elementary Steps in the Direct Synthesis of H_2O_2.

$$H_2 + 2^* \rightarrow 2H^*$$

$$O_2 + * \rightarrow O_2^*$$

$$H^* + O_2^* \rightarrow HO_2^* + *$$

$$HO_2^* + H^* \rightarrow H_2O_2^* + *$$

$$H_2O_2^* \rightarrow H_2O_2 + *$$

dx.doi.org/10.1021/cs400004y | ACS Catal. 2013, 3, 487−501

Scheme 3. Elementary Steps in the Production of H_2O during the Direct Synthesis of H_2O_2

$$O_2 + 2^* \rightarrow 2O^* \text{ or } H_2O_2^* + * \rightarrow H_2O + O^*$$

$$H^* + O^* \rightarrow HO^* + *$$

$$HO^* + H^* \rightarrow H_2O^* + *$$

$$H_2O^* \rightarrow H_2O + *$$

Competing with this reaction scheme are the reactions that lead to the undesired formation of water, which involves the hydrogenation of dissociated surface O_2 species.

In many studies, acid and halide additives are used to reduce the rates of the reactions that produce H_2O,[7−9,27,34] through reduction of the base-catalyzed decomposition of H_2O_2 and the postulated selective poisoning of catalytic hydrogenation sites by halide ions. However, in this investigation, a study will be carried out in the presence of all of the competing reactions to try to gain a greater understanding of the balance of the reactions under flow conditions. It was not intended in this study to derive a detailed kinetic model because at present, the study of the direct synthesis of H_2O_2 is in the discovery phase rather than in the process development phase. A consequence of this is that the topic draws a lot of attention in the scientific/technological community and, interestingly, many new promising catalysts are reported. Global kinetics of the direct synthesis of hydrogen peroxide in a flow system would provide an improved understanding of this complex reaction and generate new leads for research and catalysts design. The aim of the study is to investigate the use of a multiphase flow system to study the reaction parameters for the direct synthesis of H_2O_2 under flow conditions.

RESULTS AND DISCUSSION

A schematic of the flow reactor designed to test the direct synthesis of H_2O_2 is shown in Figure 1. To ensure that the reactor itself did not have significant activity toward the decomposition and hydrogenation of H_2O_2, a number of experiments were carried out to ensure H_2O_2 could pass through the system without loss due to background reactions. Aqueous H_2O_2 (4.32 wt %) was passed through the reactor, without a catalyst in place, using a range of flow rates to enable a number of contact times with the reactor to be investigated. This was necessary to determine that the reactor did not catalyze the rapid decomposition of H_2O_2. The H_2O_2 concentration was measured at the exit of the reactor after allowing 1 h for steady state to be attained. It was observed that the concentration of H_2O_2 after it had passed through the reactor remained within the experimental error of the initial concentration (shown in Supporting Information section 1). This indicates that, importantly, the reactor does not catalyze the decomposition of H_2O_2 to a great extent as it passes through the reactor in contact with the stainless steel from which the reactor is constructed.

Similar experiments were carried out in the presence of H_2 to check the hydrogenation activity of the reactor in this case in the absence of catalyst. The hydrogenation experiments showed that within experimental error, there is no loss of H_2O_2 as it passes through the reactor in the presence of H_2 at various contact times with the alloy. The same experiments were carried out using methanol as a solvent and 5 bar of 5% H_2/CO_2 to check for hydrogenation at a condition that should promote high H_2 solubility, and still, no appreciable hydrogenation activity was seen from the reactor (Supporting Information section 2).

Effect of Total Gas Flow. The effect of total gas flow rate was investigated while maintaining all other reaction conditions constant to determine the optimum total gas flow at which to carry out further reactions. The flow regime commonly observed in open channels with diameters on the order of the reactor used in this study is called Taylor flow. It consists of an alternating sequence of gas bubbles and liquid slugs, with the length of the gas bubbles being larger than the diameter of the reactor. This flow regime was confirmed by visualization experiments. When a catalyst bed was placed into the tube, the flow exited the bed still with distinct gas and liquid slugs, though less regular than Taylor flow in empty tubes. Compared with industrial trickle flow reactors, the hydrodynamics in microreactors are fundamentally different.[42] The hydrodynamics in the micropacked bed reactor are dominated by the capillary forces, resulting in high liquid hold-up values (0.65−

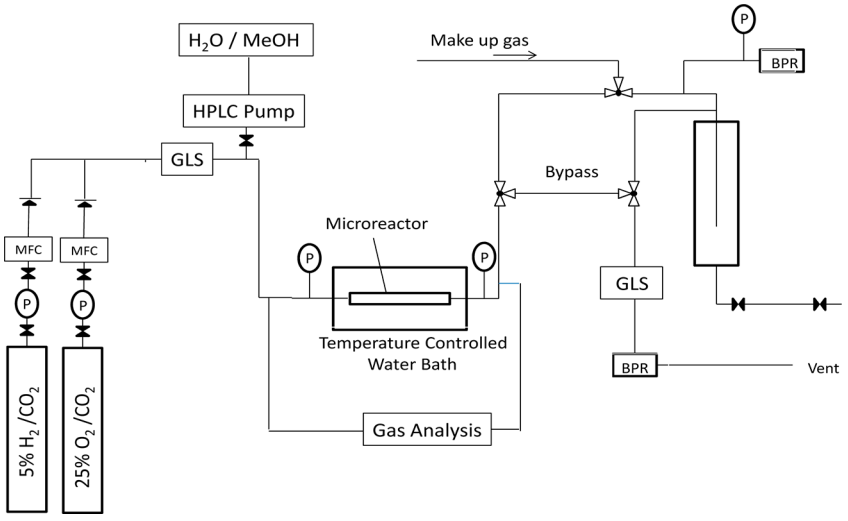

Figure 1. Schematic of the flow reactor designed to test H_2O_2 synthesis. P = pressure gauge, MFC = mass flow controller, GLS = gas liquid separator, BPR = back pressure regulator.

dx.doi.org/10.1021/cs400004y | ACS Catal. 2013, 3, 487−501

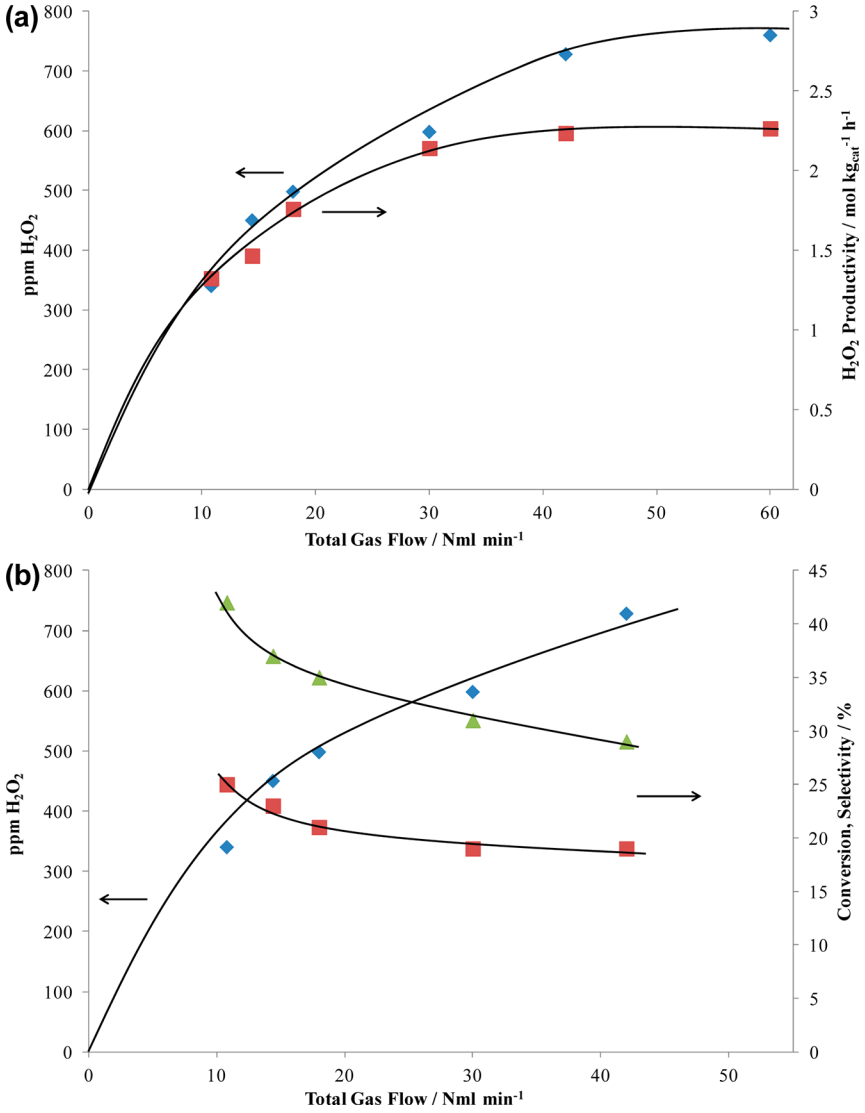

Figure 2. (a) Effect of total flow rate on the amount of H_2O_2 synthesized and the production rate of H_2O_2 while maintaining the H_2/O_2 ratio. (b) Effect of total gas flow on the amount of H_2O_2 synthesized while maintaining the H_2/O_2 ratio. H_2O_2 concentration (◇), H_2 conversion (□), and H_2O_2 selectivity (Δ). Reaction conditions: 10 bar; 2 °C; various gas flows; H_2/O_2, 1:1 (each 4%, balance CO_2); solvent, 66% MeOH/34% H_2O; liquid flow rate, 0.2 mL/min; 120 mg catalyst.

0.85).[43] The gas flow tends to flow along preferential channels, causing the existence of larger zones in which there is only liquid. An advantage of using a microreactor is the small diameter, reducing the effect of maldistribution inherent to the existence of relatively stagnant liquid zones. In the tubing upstream of the bed, the prevailing Taylor flow conditions guarantee fast mass transfer from the gas phase to the liquid phase upstream of the bed.

Experiments were carried out at increasing total gas flow rate while keeping the reactant concentrations of the feed constant together with the catalyst mass to determine the optimum gas flow rate. The importance of this was highlighted in previous studies[38,39] investigating the reaction conditions for the direct synthesis process. The H_2O_2 concentration obtained and the H_2O_2 productivity are shown in Figure 2a. As the gas flow increased, the H_2O_2 concentration that was produced also increased to a maximum of 760 ppm at 42 N mL min^{-1} total gas flow, after which point no further increase in H_2O_2 was observed with increasing gas flow.

The increase in the average rate of production of H_2O_2 with increasing gas flow rate can be explained by an increasing concentration of H_2 at the catalyst surface; two mechanisms suggest themselves. First, due to reaction, a H_2 concentration gradient over the length of the reactor is created, lowering the average reaction rate. Increasing the H_2 flow rate decreases this gradient in the liquid phase. Second, the origin of the effect could be due to the hydrodynamics determining the rate of mass transfer between the gas phase and the catalyst surface. In this process, H_2 is consumed in the H_2O_2 synthesis and in the nonselective production of H_2O. Figure 2b gives the data of the conversion and the selectivity at the varying gas flow rates. The conversion decreases with increasing gas flow rate, showing that, indeed, the concentration in the gas phase (proportional to 1 − H_2 conversion) increases along the length of the reactor. However, the change is not large, <30%, leading to an average increase in the H_2 concentration of 15%, maximally. Figure 2a shows an increase in rate of 150% between 10 and 42 N mL min^{-1} total gas flow. Thus, the effect of the lower H_2 concentration is far too low to explain the observation. When

dx.doi.org/10.1021/cs400004y | ACS Catal. 2013, 3, 487−501

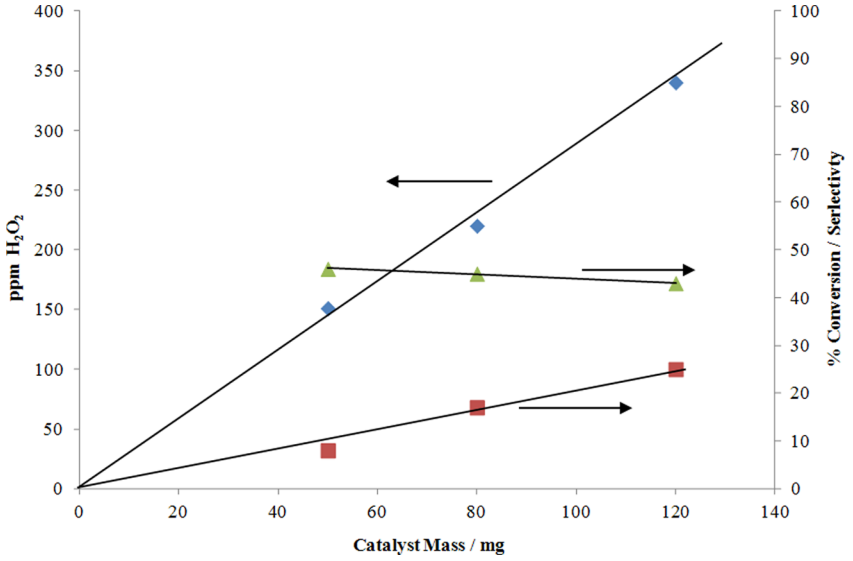

Figure 3. Effect of catalyst mass on the amount of H_2O_2 synthesized. H_2O_2 concentration (◇), H_2 conversion (□), and H_2O_2 selectivity (Δ). Reaction conditions: 10 bar; 2 °C; various gas flows; H_2/O_2, 1:1 (4% each, balance CO_2); solvent, 66% MeOH/34% H_2O; liquid flow rate, 0.2 mL/min; various catalyst masses, gas flow rates; catalyst mass, 0.11.

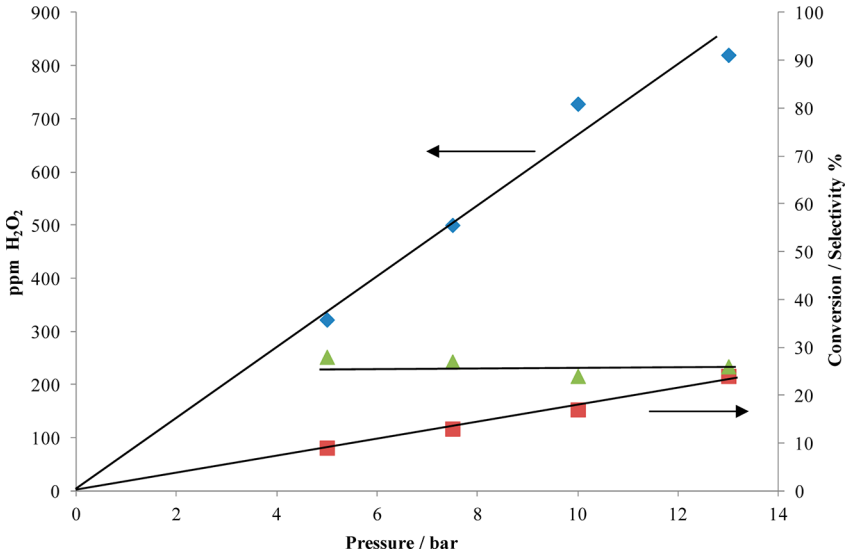

Figure 4. Effect of total pressure on the amount of H_2O_2 synthesized. H_2O_2 concentration (◇), H_2 conversion (□), and H_2O_2 selectivity (Δ). Reaction conditions: various pressures; 2 °C; 42 N mL/min gas flow; solvent, 66% MeOH/34% H_2O; liquid flow rate, 0.2 mL/min; 120 mg catalyst; H_2/O_2 = 1 (4% each, balance CO_2).

taking into account the changing selectivity, the rate increase is even much higher than 150%. We conclude that the effect is mainly of a hydrodynamic nature.

At higher gas flow rates, the mass transfer between gas and liquid will increase, but probably more important is the increase in the mass transfer through the liquid layer surrounding the catalyst surface. For Taylor flow, this has been discussed extensively by Kreutzer.[44] In our microreactor, the maldistribution due to the presence of stagnant zones will be counteracted by increasing the gas flow rate. We tentatively conclude that the increased activity shown in Figure 2a is due to this phenomenon. It is physically analogous to increasing the stirring rate in a batch reactor. At this stage, the hydrodynamics at low flow rates is not fully clear. More research is needed to unravel the hydrodynamics at these conditions. At a gas flow rate above 42 N mL min^{-1} total gas flow, the observed H_2O_2 productivity rate appears to approach a limiting value of ∼2.2 mol kg_{cat}^{-1} h^{-1}, which is of the same order of magnitude as reported by Biasi et al.[38] for monometallic Pd catalyst on a variety of supports with experiments carried out in pure MeOH as a solvent at −10 °C.

The highest reactor averaged H_2O_2 productivity achieved in the flow system is of the same order of magnitude as an almost equivalent test in our batch reactor and is reported in section 3 of the Supporting Information. This indicates that at these conditions, there are no significant external mass transfer limitations in the flow system and the results can be confidently compared with results taken from our previous studies in a batch system.[41] It should be noted that this conclusion implies that the kinetic data generated are intrinsic data. In most of this paper, the conditions have been standardized at this flow rate unless otherwise stated.

dx.doi.org/10.1021/cs400004y | ACS Catal. 2013, 3, 487−501

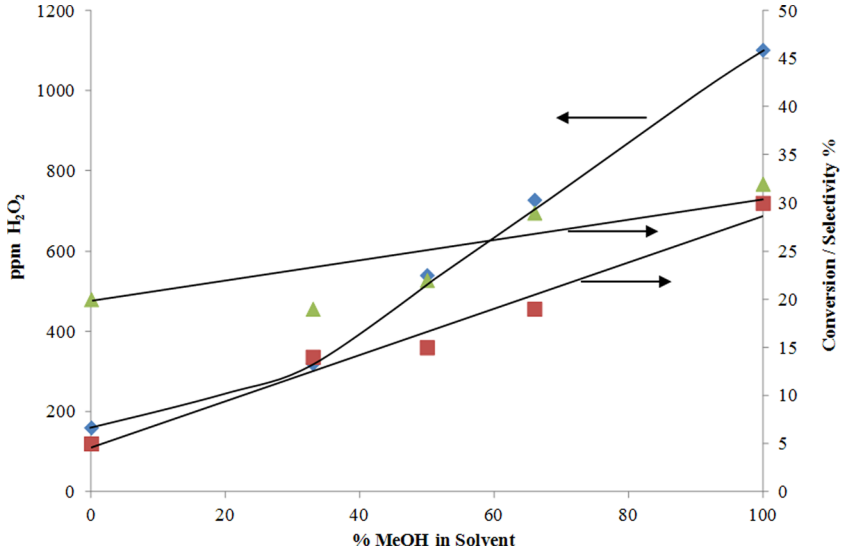

Figure 5. Effect of solvent composition on the amount of H_2O_2 synthesized, showing H_2O_2 concentration (◇), H_2 conversion (□), and H_2O_2 selectivity (Δ). Reaction conditions: 10 bar; 2 °C; 42 N mL/min gas flow; solvent, MeOH/H_2O, various ratios; flow rate, 0.2 mL/min; 120 mg catalyst; τ_{liquid}, 17.5 s; H_2/O_2 = 1 (4% each, balance CO_2).

Effect of Catalyst Mass on H_2O_2 Synthesis. The effect of catalyst mass was investigated while maintaining the other reaction variables constant, including total gas flow, pressure, temperature and H_2/O_2, with experimental details being shown in section 4 of the Supporting Information. The results are shown in Figure 3 for experiments using catalyst masses from 50 to 120 mg. The results show that as catalyst mass was increased and the gas flow adjusted to maintain a constant gas flow/catalyst mass, the concentration of H_2O_2 increased linearly with the catalyst mass. The results also show that as catalyst mass increased, H_2 conversion increased at a constant selectivity. Thus, the productivity per unit mass of catalyst is constant.

Effect of Total Pressure on H_2O_2 Synthesis. The effect of total reaction pressure was investigated in the flow system while maintaining the standard conditions. The results are shown in Figure 4. As expected, an enhancement in the H_2O_2 concentration was observed with increasing pressure, which would be expected because of higher gas solubility and smaller gas bubble size at higher pressures. As the pressure of the system increased, the H_2 conversion also increased while the selectivity of the system remained constant at ∼25%. The results show that pressure had no effect on H_2O_2 selectivity, indicating that the rate of synthesis and degradation (hydrogenation and decomposition) increase proportionately because both reactions are related to the hydrogen partial pressure. The trends of increasing productivity with increasing pressure agree with the previous observations from our investigation of reaction conditions in the batch system.[48] The trend of increasing conversion while the selectivity remains relatively constant is in contrast to Volshin's[32] work in a microreactor in which selectivity increases with increasing pressure while conversion decreases up to a pressure of 14 bar, where both conversion and selectivity remain constant on further increasing the pressure. In contrast to Volshin's study, we did not observe a decrease in H_2 and O_2 conversion with increasing pressure, which they attributed to the decrease in the direct combination of H_2 and O_2 to form water at low pressure in their reactor system.

Effect of Solvent Composition on H_2O_2 Synthesis. The effect of the solvent composition was investigated while keeping all of the other reaction conditions constant. The results are shown in Figure 5. As the methanol content in the solvent was increased, the amount of H_2O_2 produced also increased, with a maximum concentration of 1540 ppm produced in a pure methanol solvent. The increase in H_2O_2 can be explained by the increase in H_2 and O_2 solubility with increasing methanol content of the solvent. In addition, the H_2 conversion also increases with increasing methanol concentration. As the methanol content of the solvent increases, the selectivity rises slightly from ∼22% in water-only solvent to 32% in methanol only. This indicates that the rate of synthesis is higher than the rate of hydrogenation because the increase in solubility of both H_2 and O_2 will result in an enhancement in the H_2O_2 synthesis rate because it can be assumed that the reaction rate is proportional to the concentration of H_2, as previously shown when increasing the total reaction pressure.

Effect of Solvent Flow Rate on H_2O_2 Synthesis. The effect of solvent flow rate was investigated, and the results are shown in Figure 6a and b. The results for H_2O_2 concentration achieved and the total moles of H_2O_2 formed after 1 h of running the reaction at different solvent flow rates are shown in Figure 6a. The results show that as the solvent flow rate is increased, the parts per million of H_2O_2 measured decreased. Because parts per million is a measure of H_2O_2 concentration, it is expected that this would decrease with increasing solvent flow. When the moles of H_2O_2 formed were calculated, it was shown to increase with solvent flow, with a maximum at 1 mL min^{-1}. To investigate the reason for this increase in the number moles of H_2O_2 formed, the H_2 conversion and selectivity to H_2O_2 were measured and are shown in Figure 6b. The results show that at various solvent flow rates, while the moles of H_2O_2 formed increased up to 1 mL min^{-1}, the H_2 conversion remained constant at 20% while the selectivity toward H_2O_2 increased in a similar manner to the moles of H_2O_2 formed, up to a selectivity of 80%, which is comparable to high selectivities obtained with Au−Pd catalysts in other studies that report 90% selectivity at −10 °C at the same pressure.[39]

dx.doi.org/10.1021/cs400004y | ACS Catal. 2013, 3, 487−501

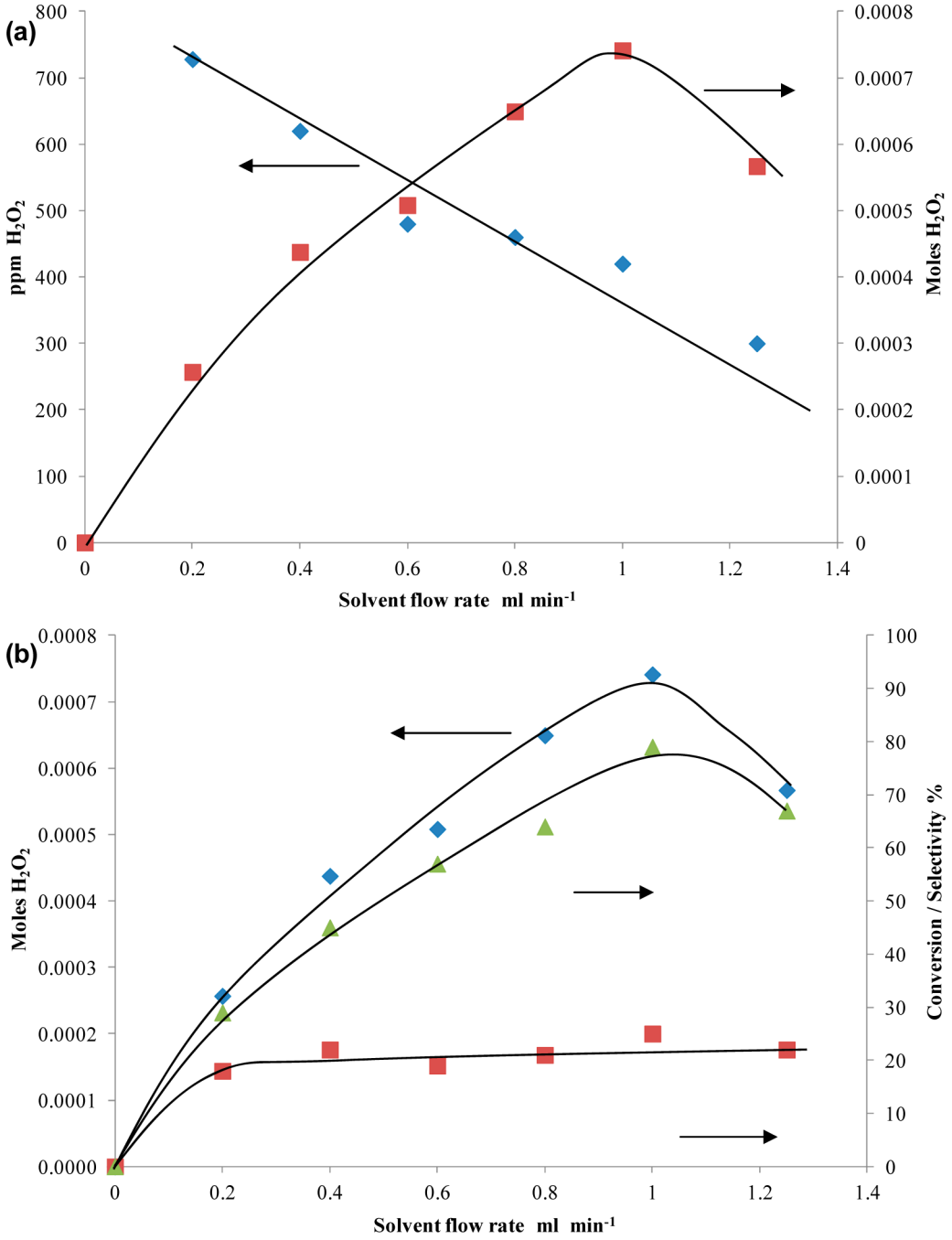

Figure 6. (a) H_2O_2 concentration obtained at various solvent flow rates, showing H_2O_2 concentration (◇) and moles of H_2O_2 formed (□). (b) H_2O_2 concentration obtained at various solvent flow rates, showing moles of H_2O_2 formed (◇), H_2 conversion (□), and H_2O_2 selectivity (Δ). Reaction conditions: 10 bar; 2 °C; 42 N mL/min gas flow; solvent, MeOH/H_2O; liquid flow rate, 0.2−1.2 mL/min; 120 mg catalyst; H_2/O_2 = 1 (4% each, balance CO_2).

On further increasing the solvent flow rate, a decrease in the amount of H_2O_2 was seen, accompanied by a drop in selectivity. The increasing selectivity at increasing solvent flow rate can be explained in terms of the residence time of the H_2O_2 formed. As more solvent is passed through the system, the residence time of H_2O_2 on the catalyst is reduced by diluting the solution. Because the extent of the subsequent hydrogenation and decomposition is proportional to the residence time of H_2O_2, the destruction of H_2O_2 by these subsequent reactions will also decrease, thereby increasing selectivity. These results confirm that hydrogenation and decomposition are still responsible for lowering the selectivity in the flow system, and the increased amount of solvent shields the synthesized H_2O_2 from the catalyst and prevents these subsequent reactions. This has implications in the challenge of making high concentrations of H_2O_2 using a catalyst that hydrogenates and decomposes H_2O_2.

Effect of Reaction Temperature on H_2O_2 Synthesis. The effect of reaction temperature was investigated, and the results are shown in Figure 7. Increasing the reaction temperature at constant gas and liquid flow rates resulted in a decrease in the H_2O_2 concentration produced during the

dx.doi.org/10.1021/cs400004y | ACS Catal. 2013, 3, 487−501

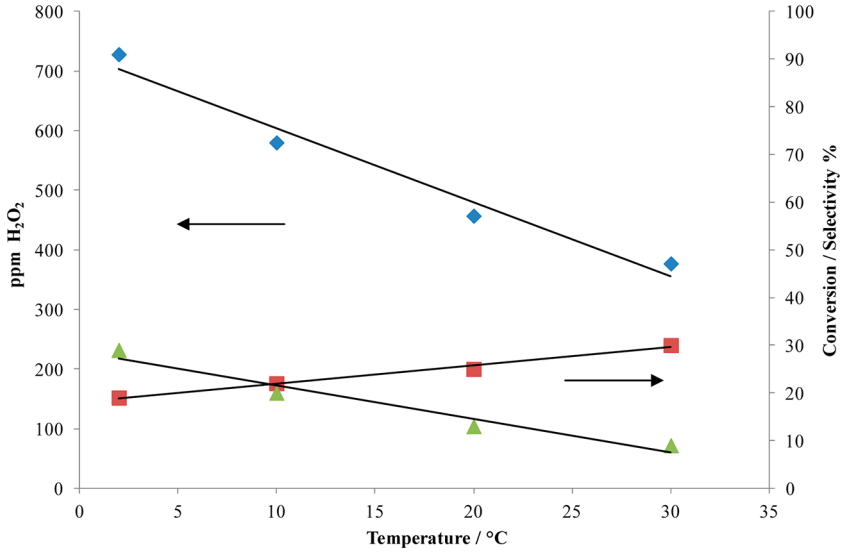

Figure 7. H_2O_2 concentration obtained at various temperatures, showing H_2O_2 concentration (◇), H_2 conversion (□), and H_2O_2 selectivity (Δ). Reaction conditions: 10 bar; various temperatures; 42 N mL/min gas flow; solvent, 66% MeOH/34% H_2O; liquid flow rate, 0.2 mL/min; 120 mg catalyst; H_2/O_2 = 1 (4% each, balance CO_2).

reaction. The experiments show that as temperature increases, the conversion of H_2 increases from 20% at 2 °C to 30% at 30 °C while the selectivity toward H_2O_2 decreases. The effect is due to the different activation energies of the synthesis reaction and subsequent degradation reactions (hydrogenation and decomposition), but the changing solubility of the reactant gases with temperature might also play a role. When the temperature of the reaction is increased, this changes the solubility of both H_2 and O_2 reactant gases in the solvent system. As the reaction temperature is increased, O_2 solubility decreases in both water (around 50% decrease when the temperature is increased from 2 to 30 °C) and methanol to a much smaller extent (around 5% decrease when the temperature is increased from 2 to 30 °C), which would reduce the rate of synthesis of H_2O_2.[45]

Conversely, the solubility of H_2 increases in methanol (by around 30% when the temperature is increased from 2 to 30 °C) at higher temperatures,[46] therefore, the rate of hydrogenation is expected to increase at higher temperatures, which will decrease H_2O_2 selectivity. It should be noted that this decrease in selectivity will be counteracted by an increase in H_2O_2 production. We conclude that the relatively high activation energy for the degradation reaction(s) is the main reason for the low H_2O_2 yield at higher temperature, confirming that if a catalyst shows appreciable degradation activity, low temperatures are desirable to obtain higher H_2O_2 concentrations. The observation by Volshin[32] using a Pd catalyst in a microreactor system that concentration of H_2O_2 increases with increasing temperature can be explained by the presence of acid and halide in the reaction solution, suppressing the subsequent hydrogenation and decompositions reactions.

The Effect of Gas Phase H_2/O_2 on H_2O_2 Concentration. The gas phase H_2/O_2 molar ratio was investigated in the flow system while all other reaction variables, including temperature, gas and liquid flow rate, pressure gas and solvent flow rate, and solvent composition, were maintained constant. Figure 8a shows that the stoichiometric 1:1 ratio was observed to be the optimum ratio to generate H_2O_2, with 760 ppm being observed. At first sight, this is surprising, because a stoichiometric composition in the gas phase does not lead to the same situation in the liquid phase. Assuming equilibrium, the ratio H_2/O_2 in the gas phase corresponds to 1:2.5 in the liquid phase consisting of 66% CH_3OH/H_2O.

As expected, the variation of this parameter was shown to have a major effect on the observed concentration of H_2O_2, with the optimum concentration being observed with equimolar gas phase concentrations. The reaction gas contains CO_2 as a diluent, which has been shown to form carbonic acid in situ by dissolving in the solvent at elevated pressure, lowering the pH of the reaction solution and increasing H_2O_2 production by making the solvent acidic and suppressing the subsequent decomposition reaction.[47] However, at a pressure of 10 bar, the solvent solution can be assumed to be saturated with CO_2, indicating that the pH of the solvent is constant throughout these experiments, and therefore, the results show the true dependence of H_2O_2 concentration on H_2/O_2 under this condition. In fact, the CO_2 content of the gas mixture increases by only ∼6% on moving from H_2/O_2 = 1 to H_2/O_2 = 0.2.

The decrease in the H_2O_2 concentration at deviation away from 1:1 can be explained in terms of the limiting reagent. Because of the available gas pressures and the lower explosive limit for H_2, the 1:1 data point is the maximum concentration of H_2 and O_2 at which a 1:1 ratio can be achieved. The data were then generated by decreasing the concentration of one of the gases, limiting the reaction by the lower reactant concentration. The total gas flow rate was kept constant at 42 N mL min^{-1} by flowing the appropriate amount of CO_2 into the system. Not taking into account the O_2 enrichment in the liquid phase due to the differing solubilities of O_2 and H_2 in the solvent mixture it might have been expected that H_2O_2 concentration would vary symmetrically around the 1:1 ratio. When the O_2 enrichment in the solvent is taken into account the opposite would be expected and an asymmetry would be expected. In fact, as has already been seen in a similar study of an Au−Pd/TiO_2 catalyst carried out in a batch system there is an asymmetry, with H_2O_2 concentration decreasing more rapidly with decreasing O_2 partial pressure than with decreasing H_2 partial pressure.[48] This can be observed more clearly when H_2/O_2 and O_2/H_2 are plotted together in Figure 8b. As shown

dx.doi.org/10.1021/cs400004y | ACS Catal. 2013, 3, 487−501

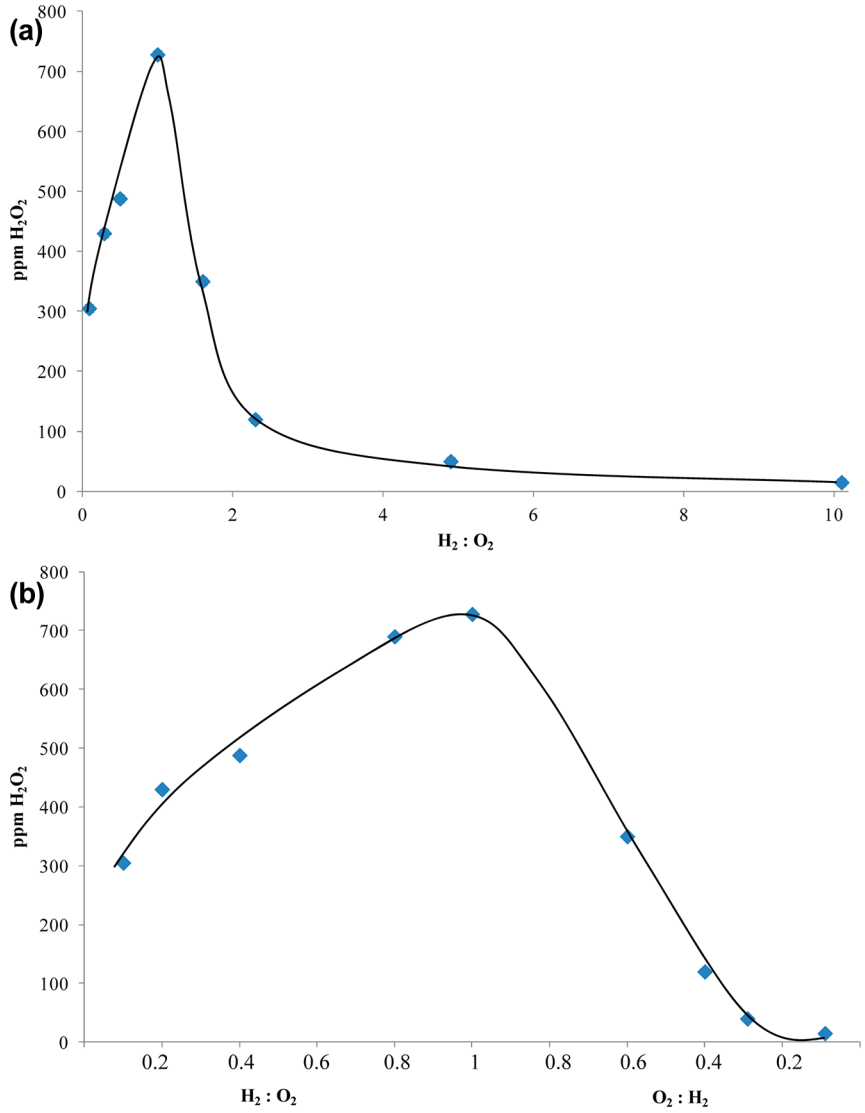

Figure 8. (a) H_2O_2 concentration obtained at various H_2/O_2. (b) H_2O_2 concentration obtained at various gas phase H_2/O_2 and O_2/H_2 ratios. Reaction conditions: 10 bar; 2 °C; 42 N mL/min gas flow; solvent, 66% MeOH/34% H_2O; liquid flow rate, 0.2 mL/min; 120 mg catalyst; τ_{liquid}, 17.5 s.

in the figure, even when at constant O_2 concentration, the concentration of H_2 is reduced by a factor of 10. This gives rise to a decrease in H_2O_2 concentration of only from 760 to 300 ppm, whereas with H_2 constant and 10 times less O_2, only around 20 ppm is observed.

These results are similar to the result seen in the batch system and can be explained in much the same way by considering the key reaction steps involved. The high dependence on pH_2 was also seen in a microreactor system[32] and studies by Biasi et al.[39] As has been previously postulated,[48] all of the reactions steps share the same intermediate reaction species, and H_2O_2 is formed by a 2-step hydrogenation of adsorbed O_2. Competing with this reaction are the reactions that lead to the undesired formation of water, which involve the hydrogenation of dissociated surface O species. The asymmetry in Figure 8b is predicted by this model in that when the H_2 partial pressure is low compared to with O_2, the concentration of the adsorbed H* will be low, meaning that less adsorbed O* will be scavenged from the catalyst surface, and therefore, less hydrogenation and decomposition will take place. In terms of kinetic equations in which the rate of hydrogenation is proportional to the H_2 partial pressure, a lower hydrogenation rate would also be predicted when O_2 is in excess as well as a lower synthesis rate. If a catalyst that showed no hydrogenation activity was tested, a much more symmetrical shape would be expected when investing H_2/O_2. This was observed using a Au−Pd/C catalyst with a lower H_2O_2 degradation rate in a batch system using various H_2/O_2 ratios.[49]

H_2O_2 Decomposition Reaction. The decomposition reaction rate was studied by pressurizing the system to 10 bar with CO_2 and maintaining a flow of 42 N mL min^{-1} total gas flow through the system. A water−methanol solvent mixture identical to that used in the synthesis experiments containing varying amounts of H_2O_2 was passed through the reactor with and without a catalyst in place to determine more accurately the background activity of the reactor under reaction conditions. Assuming that the decomposition reaction is first-order with H_2O_2, the rate can be described by the expression in eq 1.

$$\text{decomposition rate} = r_d = k_d[H_2O_2] \quad (1)$$

dx.doi.org/10.1021/cs400004y | ACS Catal. 2013, 3, 487−501

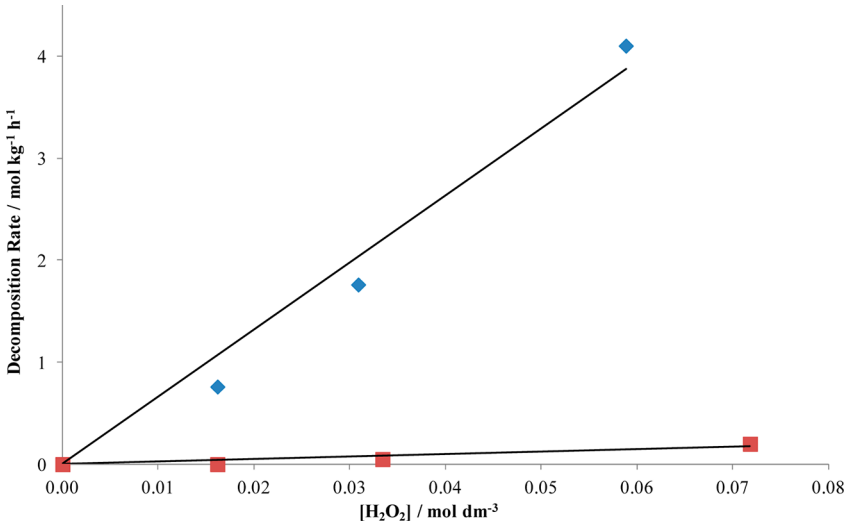

Figure 9. Effect of H_2O_2 concentration on the decomposition rate of both the catalyst and the reactor: with catalyst (◇) and without catalyst (□). Reaction conditions: 10 bar; 2 °C; 42 N mL/min CO_2 flow; solvent, 66% MeOH/34% H_2O; liquid flow rate, 0.2 mL/min; 120 mg catalyst; τ_{liquid}, 17.5 s; [H_2O_2], 0−2000 ppm.

On the basis of this expression, the decomposition rate should increase linearly as the concentration of H_2O_2 increases and should be independent of the total pressure of the system. Figure 9 shows the observed decomposition rate as a function of H_2O_2 concentration in the feed for both the catalyst and the reactor. From these data, it is clear to see that the reactor contributes only a small amount to the decomposition activity. From these data, it is possible to obtain a pseudo-first-order rate constant for the catalyst at the reaction condition investigated. The gradient of this line gives this rate constant for the decomposition reaction, which equals 68 $dm^3\ kg^{-1}\ h^{-1}$. It is appreciated that for establishing a real intrinsic kinetic model, more data are needed, allowing a correct description of this integral reactor. However, for the purpose of this study, the data found can be applied in the range of the reaction conditions used. To confirm that the decomposition reaction was independent of pressure, the experiment was repeated at various pressures of CO_2 in the presence of the catalyst, and the decomposition rate remained constant between 2 and 15 bar.

H_2O_2 Hydrogenation Reaction. The hydrogenation kinetics were studied by pressurizing the reactor with H_2 and CO_2 at various concentrations while maintaining the gas flow rate and also by passing various concentrations of H_2O_2 through the system at constant H_2 concentration and measuring the hydrogenation rate. The observed rate during these experiments is a combination of the hydrogenation and decomposition rates, so to extract the hydrogenation rate, the decomposition rate at the reaction condition was subtracted from the observed rate, assuming that decomposition and hydrogenation are independent parallel processes. Assuming that the hydrogenation reaction rate is first-order with H_2O_2 and H_2, it can be described by eq 2.

$$\text{hydrogenation rate} = r_h = k_h[H_2][H_2O_2] \quad (2)$$

By holding one of the reactants constant while varying the other, it is possible to determine k_h in two ways: by varying [H_2O_2] while maintaining [H_2] and vice versa. Figure 10a shows how the average hydrogenation rate varies linearly with increasing [H_2] in the feed at constant [H_2O_2] for the catalyst and an empty reactor tube. From these data, a pseudo rate constant can be extracted from the gradient of the graph, which is equal to $k_h[H_2O_2]$; from these data, a value of k_h of 1130 $dm^6\ kg^{-1}\ h^{-1}\ mol^{-1}$ can be obtained. From the results, it is seen that the reactor has a small amount of hydrogenation activity but minimal when compared with the catalyst. To verify the results, the same experiment was conducted, but this time varying the H_2O_2 concentration, shown in Figure 10b. From these data, a pseudo rate constant can be extracted from the gradient of the graph, which is equal to $k_h[H_2]$. From these data, a value of k_h of 1080 $dm^6\ kg^{-1}\ h^{-1}\ mol^{-1}$ can be obtained, which is in good agreement with the value obtained previously by varying the concentration of H_2.

Comparing the rates of decomposition and hydrogenation, it is clear that the former is the higher. It should be noted that this does not mean that H_2O_2 conversion into H_2O is faster in an inert atmosphere than in a H_2 atmosphere. The hydrogenation data have been corrected for the decomposition, and strictly speaking, they represent the additional conversion when changing the gas phase into an H_2 atmosphere. This interpretation is in full agreement with earlier work carried out in the group.[20]

Kinetic Analysis of Synthesis Reaction. As was shown previously, the concentration of H_2O_2 synthesized does not depend symmetrically on the H_2/O_2. Because of the H_2O_2 hydrogenation rate being proportional to the concentration of H_2, it is expected that increasing the H_2 in the system (at constant O_2) decreases the observed H_2O_2 concentration more rapidly than an increase in O_2 (at constant H_2). Increasing the O_2 concentration in the system increases the synthesis rate without increasing the hydrogenation rate. Because of the available gas cylinders, the O_2 concentration could not be increased past the values used to obtain the maximum H_2O_2 concentration shown earlier, [O_2] = 4 vol %.

To model the synthesis reaction, a rate synthesis constant must be determined for both the O_2 and H_2 rich system. This was done by initially starting from H_2/O_2 = 1:1 and gradually decreasing one of the reactants while maintaining the concentration of the other. Following from the analysis of the decomposition and hydrogenation reactions, a similar kinetic expression can be used to estimate the gross H_2O_2 synthesis rate. Because it is not possible to measure the gross H_2O_2 synthesis rate in the absence of promoters because of the

dx.doi.org/10.1021/cs400004y | ACS Catal. 2013, 3, 487−501

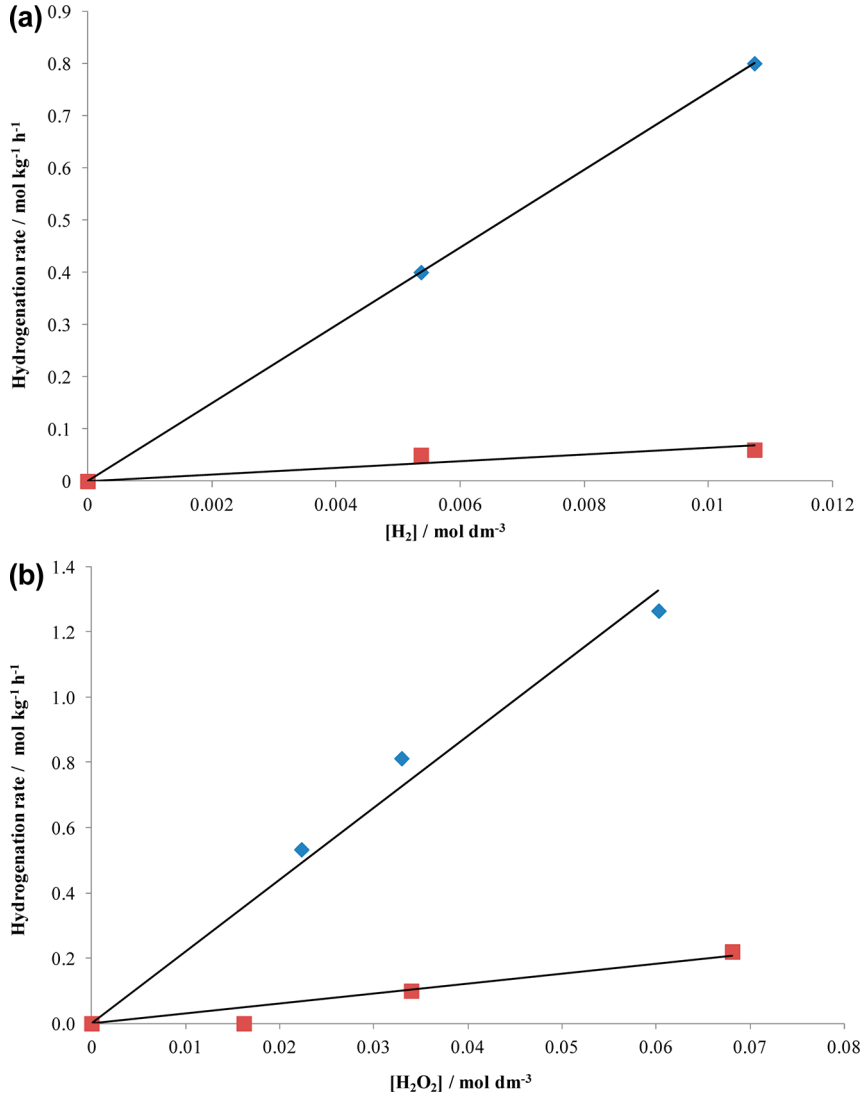

Figure 10. (a) Effect of H_2 concentration on the hydrogenation rate of both the catalyst and the reactor corrected for decomposition rate: with catalyst (◊), without catalyst (□). (b) Effect of H_2O_2 concentration on the hydrogenation rate of both the catalyst and the reactor corrected for decomposition rate: with catalyst (◇) and without catalyst (□). Reaction conditions: 10 bar; 2 °C; 42 N mL/min gas flow; solvent, 66% MeOH/34% H_2O; liquid flow rate, 0.2 mL/min; 120 mg catalyst; τ_{liquid}, 17.5 s; $[H_2]$, 4 vol %.

hydrogenation and decomposition reactions always competing with the synthesis reaction, an estimate can be made using eqs 3−5. The gross rate at which H_2O_2 is formed can be estimated on the basis of the net synthesis rate and the degradation rate shown in eqs 3 and 4, where the decomposition and hydrogenation have been grouped into one term to describe H_2O_2 degradation.

$$r_s^{net} = r_s^{gross} - r_{deg} \quad (3)$$

$$r_s^{gross} = r_s^{net} + k_{deg}[H_2][H_2O_2] \quad (4)$$

$$r_s^{gross} = r_s^{net} + k'_{deg}[H_2O_2] \quad (5)$$

From inspection of the degradation rates response to $[H_2O_2]$ and $[H_2]$, it was seen that the response was first-order with respect to $[H_2O_2]$ (shown in Supporting Information section 5). The degradation rate showed much less dependence on $[H_2]$, indicating that the degradation rate is very sensitive to $[H_2O_2]$ and not $[H_2]$, which suggests that the major degradation reaction is decomposition. To calculate the gross synthesis rate, it was assumed that the degradation rate was zero-order with respect to $[H_2]$. The equation used to estimate the gross synthesis rate is shown as eq 5. An additional assumption used to aid in the simplicity of the analysis was to use the final observed $[H_2O_2]$ measured at the exit of the reactor to calculate the gross rate of H_2O_2 synthesis. Without very detailed experimental work, the gross $[H_2O_2]$ cannot be determined, which is needed to accurately calculate the degradation rate. Because we have measured $[H_2O_2]$ at the exit of the reactor, this represents the maximum degradation rate. The implication of this is that the real degradation rate is overestimated, and as a consequence, the gross synthesis rate is underestimated.

The effect of reducing the O_2 content in the reaction and, therefore, carrying out the reaction in a H_2-rich atmosphere is shown in Figure 11a. It can be observed that the synthesis rate depends linearly on the O_2 concentration and therefore can be assumed to be first-order with respect to O_2, with a gradient of 223 $dm^6\ kg^{-1}\ h^{-1}\ mol^{-1} = k_s[H_2]$. Therefore, k_s = 11 730 $dm^6\ kg^{-1}\ h^{-1}\ mol^{-1}$ when H_2 is in excess. The effect of reducing the

dx.doi.org/10.1021/cs400004y | ACS Catal. 2013, 3, 487−501

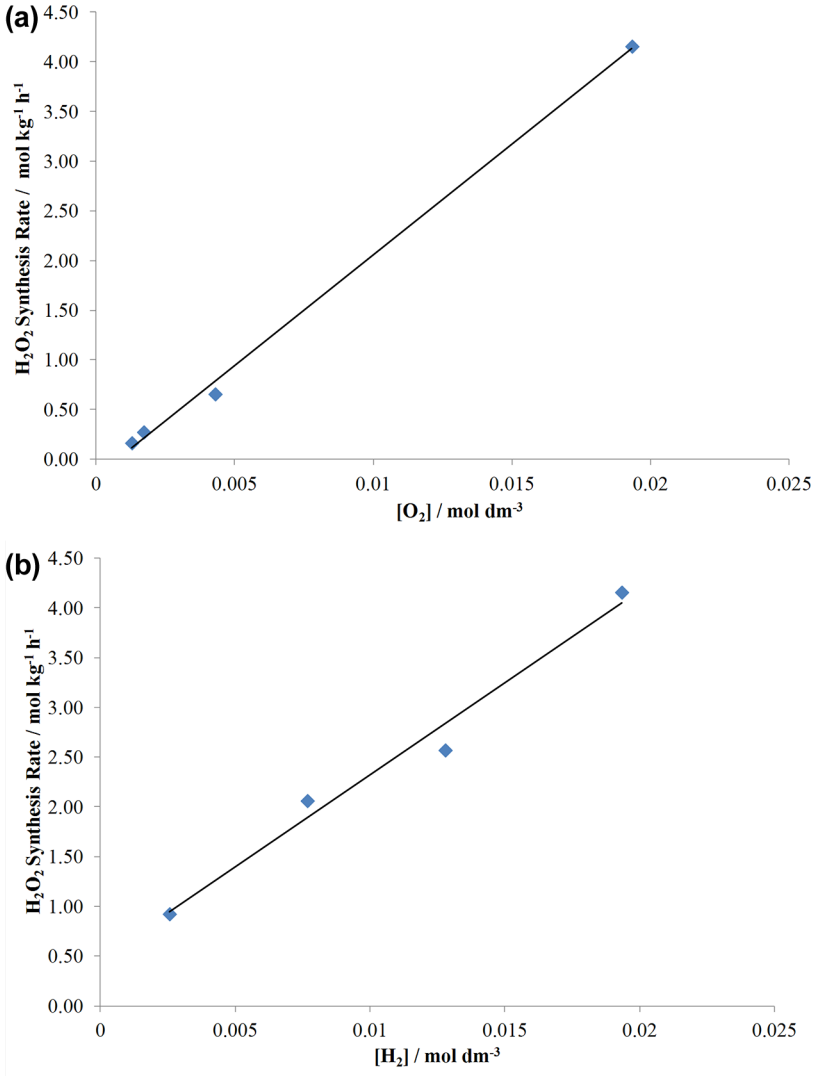

Figure 11. (a) Effect of O_2 concentration on the estimated gross synthesis rate (◇). (b) Effect of H_2 concentration on the estimated gross synthesis rate (◊). Reaction conditions: 10 bar; 2 °C; 42 N mL/min gas flow; solvent, 66% MeOH/34% H_2O; solvent flow rate, 0.2 mL/min; 120 mg catalyst; τ_{liquid}, 17.5 s; $[O_2]$, 0.017 mol dm^{-3}.

H_2 content in the reaction and therefore carrying out the reaction in an O_2-rich atmosphere is shown in Figure 11b. It can be seen that the synthesis rate depends linearly on the H_2 concentration and, therefore, can be assumed to be first-order with respect to H_2, with the gradient of the graph being 185 $dm^6\ kg^{-1}\ h^{-1}\ mol^{-1} = k_h[O_2]$. Therefore, k_s = 9750 $dm^6\ kg^{-1}\ h^{-1}\ mol^{-1}$ when O_2 is in excess. As shown in Figure 8b, $[H_2O_2]$ decreases more rapidly when H_2 is in excess compared with when O_2 is in excess. This is shown in the estimated gross synthesis rate constants being higher for the condition that H_2 is in excess and the concentration of O_2 is systematically reduced.

The experiments carried out have allowed rate constants to be determined for all of the reactions that are taking place in the direct synthesis process and are summarized below. It is important to note that these quasi rate constants are related to the standard experimental conditions used.

$$k_d = 63\ dm^3\ kg^{-1}\ h^{-1}$$

$$k_h = 1130\ dm^6\ kg^{-1}\ h^{-1}\ mol^{-1}$$

$$k_s = 11730\ dm^6\ kg^{-1}\ h^{-1}\ mol^{-1} \quad \text{when } H_2 \text{ is in excess}$$

$$k_s = 9750\ dm^6\ kg^{-1}\ h^{-1}\ mol^{-1} \quad \text{when } O_2 \text{ is in excess}$$

Combining Experimental Results To Form a Global Kinetic Model for the Direct Synthesis of Hydrogen Peroxide. From the experiments carried out so far, it has been possible to establish in a semiempirical way a kinetic model including quasi rate constants for the H_2O_2 decomposition reaction, hydrogenation reaction, and the synthesis reaction, in both an O_2-rich and H_2-rich environment using this catalyst under our reaction conditions.

Figure 12 shows a comparison among the measured net synthesis rate, degradation rate, and the calculated gross synthesis rate for various H_2/O_2 ratios. This plot indicates that there is a large amount of degradation; in fact, the degradation rate is similar in magnitude to the net synthesis rate, which indicates that the actual amount of H_2O_2 synthesized is much higher than the observed concentrations measured during the reactions.

Following this, using the pseudo rate constants obtained for the degradation, hydrogenation, and decomposition reactions,

dx.doi.org/10.1021/cs400004y | ACS Catal. 2013, 3, 487−501

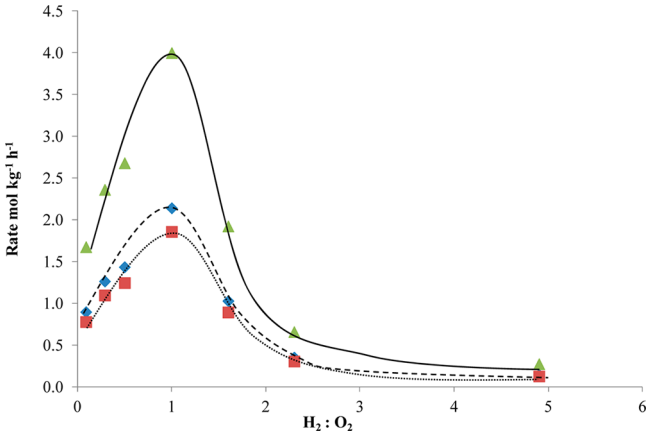

Figure 12. Plot to compare the net synthesis rate (◇), degradation rate (□), and calculated gross synthesis rate (Δ). Reaction conditions: 10 bar; 2 °C; 42 N mL/min gas flow; H_2/O_2, various; solvent, 66% MeOH/34% H_2O; flow rate, 0.2 mL/min; 120 mg catalyst; τ_{liquid}, 17.5 s.

it is possible to use the rate equations for each reaction to evaluate the relative contribution of H_2O_2 decomposition and hydrogenation to the overall degradation rate at various H_2/O_2 ratios. This is shown in Figure 13. When comparing the rates of

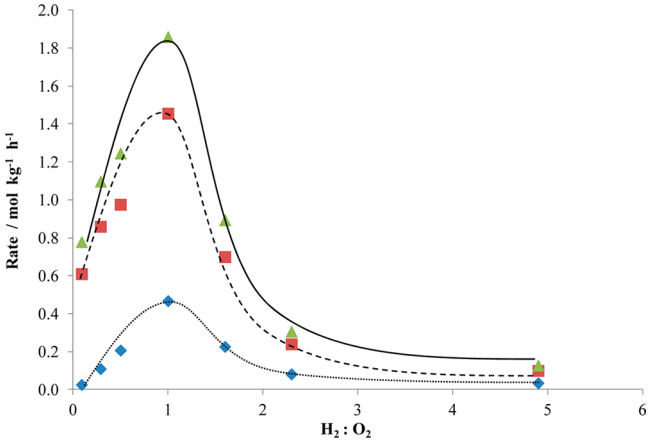

Figure 13. Rates of H_2O_2 degradation, hydrogenation, and decomposition rate at various H_2/O_2 ratios using the obtained pseudo rate constants. H_2O_2 degradation rate (Δ), decomposition (□), and hydrogenation (◇). Reaction conditions: 10 bar; 2 °C; 42 N mL/min gas flow; H_2/O_2, various; solvent, 66% MeOH/34% H_2O; flow rate, 0.2 mL/min; 120 mg catalyst; τ_{liquid}, 17.5 s.

the subsequent reactions, it was observed that the decomposition reaction has a much higher rate than the hydrogenation reaction. At the point of maximum synthesis rate, $H_2/O_2 = 1$, the net synthesis rate is equal to 2.2 mol kg_{cat}^{-1} h. The decomposition reaction rate is relatively close to this value at 1.6 mol kg_{cat}^{-1} h^{-1}, whereas the hydrogenation rate is almost 3 times as low at 0.5 mol kg_{cat}^{-1} h^{-1}.

The results suggest that although the absence of hydrogenation will increase the amount of H_2O_2 slightly, the subsequent reaction that has the highest rate in this reactor setup is the decomposition reaction. This indicates that to make higher concentrations of H_2O_2 in a flow reactor system using this catalyst, it is the decomposition reaction that has the greater limiting effect on the yield of H_2O_2, and this should be addressed either through further catalyst design or engineering developments. It is shown in Figure 13 that the rate of decomposition is much higher than the rate of hydrogenation. As speculated earlier, this means that the degradation of H_2O_2 (combination of hydrogenation and decomposition) is not very strongly influenced by H_2 concentration because of the much higher decomposition rate, assuming that hydrogenation and decomposition are independent, parallel process.

The observation that decomposition is the limiting sequential reaction of hydrogen peroxide in this system is in contrast with studies that claim that hydrogenation is the limiting reaction;[36] however, the previous work was carried out in a batch reactor where residence times of the gas and liquid with the catalysts are much longer. This observation has been corroborated in our own batch reactors, where reactions conducted for 30 min at 10 bar of 5% H_2/CO_2 and 25% O_2/CO_2 at the same ratio used in the optimum flow experiments and using identical solvent compositions showed that the hydrogenation rate was twice the decomposition rate. The results of our study show that using the flow reactor system to obtain very short residence times greatly decreases the contribution of hydrogenation during the direct synthesis process using this catalyst; however, the decomposition reaction is not so affected and, consequently, becomes more important.

In terms of elementary steps associated with the synthesis reaction, to achieve high concentrations, O_2 and H_2O_2 should preferably not be exposed to neighboring empty sites, which can dissociate O−O bonds. Designing catalysts without these sites should be the focus of further catalytic design studies.

In addition, it should be noted that the selectivity of H_2O_2 production is roughly 25%. Thus, 75% of the H_2 is consumed in the direct production of water, through either hydrogenation or subsequent decomposition. In this undesired reaction, dissociation of O_2 or H_2O_2 is the cause of the low selectivity.[20] Thus, catalysts should be developed that do not catalyze O−O dissociation in either molecular O_2 or H_2O_2.

CONCLUSIONS

H_2O_2 synthesis has been carried out in a small-scale, fixed-bed reactor to investigate how reaction conditions affect the concentration achievable. Reaction conditions, including pressure, temperature, residence time, solvent composition, and solvent flow, have been studied and have been shown to have marked effects on the amount of H_2O_2 measured. Investigation into the H_2O_2 decomposition and hydrogenation reactions have been carried out, and it has been shown that they can be described by simple kinetic equations. Combined with the synthesis reaction, a simple kinetic model that takes into account all of the competing and subsequent reactions has been described. Using this model, it can be shown that the decomposition reaction has the most significant effect on the amount of H_2O_2 formed, not the hydrogenation reaction. The global kinetic model derived suggests the development of catalysts with minimal O−O dissociation rates should be the focus of future catalyst design and engineering studies.

EXPERIMENTAL SECTION

Catalyst Preparation. H_2O_2 synthesis/hydrogenation/decomposition experiments were carried out using a 0.5% Au/0.5% Pd/TiO_2 catalyst prepared by impregnation and reduced at 400 °C/4 h with a ramp rate of 10 °C min^{-1}. This catalyst was developed using a modified impregnation procedure that we have recently reported. This catalyst was

dx.doi.org/10.1021/cs400004y | ACS Catal. 2013, 3, 487−501

selected so as to avoid any metal leaching during the extended testing runs because it has a low metal content and was shown to be stable in previous studies.[41] This catalyst was pressed into a disk and sieved to a particle size of 425−250 μm for catalytic tests in the flow system.

Catalyst Testing. A continuous, fixed-bed rector was constructed for the direct synthesis of H_2O_2 using Swagelok fittings with an internal diameter of 1/8 in. to minimize the volume of gas in the system and to ensure safety. Gas flows of 5% H_2/CO_2 and 25% O_2/CO_2 were controlled using mass flow controllers (MFCs), and the pressure was maintained using a back-pressure regulator at the end of the system; pressure relief valves were included at various points throughout the system. Solvent, typically water/MeOH containing no acid or halide additives, was pumped through the system using an HPLC pump, a gas liquid separator (GLS), and one-way valves were placed after the MFCs to prevent any liquid from entering the MFCs during the reaction. Pressure gauges were placed before and after the catalyst bed to monitor the pressure drop through the bed and to indicate if a blockage had formed in the system. Liquid was collected downstream before the back-pressure regulator by emptying a 150 mL GLS fitted with a valve which acted as a sample bomb. A schematic of the reactor is shown in Figure 1.

A typical H_2O_2 synthesis reaction was carried out using between 50 and 120 mg of 1% $AuPd/TiO_2$, which had been pressed into a disk and sieved to a particle size of 425−250 μm. The sample was supported at the bottom of the catalyst bed in the reactor tube by glass wool. The catalyst was contained within a 10 cm stainless steel tube with an internal diameter of 1/8 in. This resulted in a catalyst bed length of around 4 cm when 120 mg of catalyst was used, which was typical for most experiments, unless specified. The reactor system was then pressurized, typically to 10 bar, with a 1:1 mixture of H_2 and O_2 from the respective CO_2 diluted cylinders. The Brooks MFC used to supply the flow of 5% H_2/CO_2 had a range of 0−200 N mL min^{-1}, and the MFC used to supply the 25% O_2/CO_2 had a flow range of 0−50 N mL min^{-1}. The reactor was then cooled by the water bath to 2 °C. When the reactor had reached pressure and the flow through the system had stabilized, the solvent flow (typically, 0.2 mL min^{-1}) was introduced into the system. Both gas and liquid flowed concurrently through the catalyst bed from top to bottom. Liquid samples were taken from the sample bomb every 60 min, and the concentration of H_2O_2 was determined by titration against an acidified dilute $Ce(SO_4)$ solution using ferroin as an indicator. During the study, the amount of H_2O_2 was quoted as either the concentration formed in the reaction solution in units of parts per million (ppm) or as the observed rate of reaction/productivity in units of moles per kilogram of catalyst per hour (mol kg_{cat}^{-1} h^{-1}).

The residence time of the gas through the catalyst bed was calculated using the gas phase volume of the catalyst bed and the gas flow rate. The empty volume in the reactor was estimated to be 40%, and the liquid hold-up, 80% of the empty volume.[42] $\tau_{gas} = V_{gas}$/gas flow rate.

$$V_{Gas} = \text{empty volume fraction} \times \text{reactor volume}$$
$$= 0.4 \times 0.2 \times \text{reactor volume}$$

The liquid residence time is defined analogously.

The productivity is defined as the number of moles of H_2O_2 produced per kilogram of catalyst per hour and is determined by titration of the reaction solution after 1 h of the reaction running.

H_2O_2 hydrogenation experiments were carried out in the flow reactor by replacing the 25% O_2/CO_2 feed with 100% CO_2 while maintaining the flow rate through the catalyst bed. As a solvent, 500 ppm H_2O_2 in H_2O/MeOH solution was passed through the catalyst, and by titrating the solution before and after passing through the catalyst bed, it is possible to determine loss in H_2O_2 due to hydrogenation and decomposition.

H_2O_2 decomposition experiments were carried out by replacing both the H_2 and O_2 feeds with 100% CO_2 and passing H_2O_2 solution through the catalyst and determining the loss in H_2O_2 by titration.

A Varian 3800 GC fitted with a TCD was used to analyze the gas stream exiting the H_2O_2 flow reactor. The GC was fitted with a 3 m molecular sieve 5 Å column and argon used as a carrier gas at a flow rate of 30 N mL min^{-1}. As an internal standard 1% of the total gas flow was N_2, which provided a reference to compare the ratio of H_2 and O_2 before and after the reaction. The column oven was held at 40 °C for 6 min, which allowed separation of H_2, O_2, and N_2. The oven was then ramped at 25 °C min^{-1} up to 200 °C to ensure all CO_2 and moisture was removed from the column. H_2 conversion was measured by comparing the concentration of H_2 before and after the reaction. Selectivity toward H_2O_2 was measured by calculating the number of moles of H_2O_2 synthesized over a set period of time compared with the number of moles of H_2 converted over the same time period.

SAFETY

To ensure the safety of the reactor in contacting a H_2/O_2 mix, it is essential to ensure the gas composition remains below the lower explosive limit of H_2, 5% in air at room temperature. This is ensured by using intrinsically safe gas mixtures of 5% H_2/CO_2, 25% O_2/CO_2. Although the reaction is exothermic, hot spots in the reactor are minimized by cooling the reactor throughout the reaction with a water bath. The other major safety issue is a rapid pressure increase due to a blockage in the system, which could cause a failure in one of the reactor joints. The risk of this is controlled by fitting pressure relief valves before and after the catalyst bed. In addition, MFC inlet pressures of 15 bar are used, which means that once the pressure of the reactor has equaled the inlet pressure of the MFCs, no more gas will flow into the system.

ASSOCIATED CONTENT

Supporting Information

Results of the initial decomposition and hydrogenation reactions of H_2O_2 and the reactor alloy and the results of testing of the pelleted catalyst in a batch reactor. This material is available free of charge via the Internet at http://pubs.acs.org.

AUTHOR INFORMATION

Corresponding Author

*Phone: (+44) 29 2087 4059. Fax: (+44) 2920-874-030. E-mail: hutch@cardiff.ac.uk.

Author Contributions

The experimental work was conducted by S.J.F. and assisted by M.P. J.K.E. and E.N.N. helped supervise the work. J.A.M. aided in the design of the kinetic model. The work was directed by G.J.H. The paper was written by S.J.F., J.A.M., and G.J.H.

Notes

The authors declare no competing financial interest.

■ ACKNOWLEDGMENTS

We thank Cardiff University and the EPSRC for financial support.

■ REFERENCES

(1) Campos-Martin, J. M.; Blanco-Brieva, G.; Fierro, J. L. G. *Angew. Chem., Int. Ed.* **2006**, *45*, 6962−6984.
(2) Corti, C. W.; Holliday, R. J.; Thompson, D. T. *Appl. Catal., A* **2005**, *291*, 253−261.
(3) Choudhary, V. R.; Samanta, C.; Choudhary, T. V. *Appl. Catal., A* **2006**, *308*, 128−133.
(4) Liu, Q. S.; Lunsford, J. H. *J. Catal.* **2006**, *239*, 237−243.
(5) Chinta, S.; Lunsford, J. H. *J. Catal.* **2004**, *225*, 249−255.
(6) Chinta, S.; Lunsford, J. H. *Abstr. Papers Am. Chem. Soc.* **2004**, *227*.
(7) Choudhary, V. R.; Samanta, C.; Jana, P. *Appl. Catal., A* **2007**, *317*, 234−243.
(8) Choudhary, V. R.; Samanta, C.; Choudhary, T. V. *Catal. Commun.* **2007**, *8*, 1310−1316.
(9) Choudhary, V. R.; Jana, P. *Catal. Commun.* **2008**, *9*, 1624−1629.
(10) Colery, J.; Schoebrechts, J.; Van Weynbergh, J. U.S. Patent 5,447,706, 1995.
(11) Edwards, J. K.; Solsona, B.; Landon, P.; Carley, A. F.; Herzing, A.; Kiely, C. J.; Hutchings, G. J. *J. Catal.* **2005**, *236*, 69−79.
(12) Edwards, J. K.; Solsona, B.; Landon, P.; Carley, A. F.; Herzing, A.; Watanabe, M.; Kiely, C. J.; Hutchings, G. J. *J. Mater. Chem.* **2005**, *15*, 4595−4600.
(13) Edwards, J. K.; Thomas, A.; Carley, A. F.; Herzing, A.; Kiely, C. J.; Hutchings, G. J. *Green Chem.* **2008**, *10*, 388−394.
(14) Edwards, J. K.; Hutchings, G. J. *Angew. Chem., Int. Ed.* **2008**, *47*, 9192−9198.
(15) Edwards, J. K.; Solsona, B.; Ntainjua, N. N.; Carley, A. F.; Herzing, A. A.; Kiely, C. J.; Hutchings, G. J. *Science* **2009**, *323*, 1037−1041.
(16) Li, G.; Edwards, J. K.; Carley, A. F.; Hutchings, G. J. *Catal. Today* **2006**, *114*, 369−371.
(17) Solsona, B. E.; Edwards, J. K.; Landon, P.; Carley, A. F.; Herzing, A.; Kiely, C. J.; Hutchings, G. J. *Chem. Mater.* **2006**, *18*, 2689−2695.
(18) Ntainjua, N. E.; Piccinini, M.; Pritchard, J. C.; He, Q.; Edwards, J. K.; Carley, A. F.; Moulijn, J. A.; Kiely, C. J.; Hutchings, G. J. *Chem. Cat. Chem.* **2009**, *1*, 479−484.
(19) Bernardotto, G.; Menegazzo, F.; Pinna, F.; Signoretto, M.; Cruciani, G.; Strukul, G. *Appl. Catal., A* **2009**, *358*, 129−135.
(20) Ntainjua, N.; Edwards, E.; Carley, J. K.; Lopez-Sanchez, A. F.; Moulijn, J. A.; Herzing, A. A.; Kiely, C. J.; Hutchings, G. J. *Green Chem.* **2008**, *10*, 1162−1169.
(21) Edwards, J. K.; Thomas, A.; Solsona, B. E.; Landon, P.; Carley, A. F.; Hutchings, G. J. *Catal. Today* **2007**, *122*, 397−402.
(22) Edwards, J. K.; Ntainjua, E.; Carley, A. F.; Herzing, A. A.; Kiely, C. J.; Hutchings, G. J. *Angew. Chem., Int. Ed.* **2009**, *48*, 8512−8515.
(23) Li, J.; Ishihara, T.; Yoshizawa, K. *Phys. Chem. C* **2011**, *115*, 25359−25367.
(24) Abate, S.; Melada, S.; Centi, G.; Perathoner, S.; Pinna, F.; Strukul, G. *Catal. Today* **2006**, *117*, 193−198.
(25) Abate, S.; Centi, G.; Melada, S.; Perathoner, S.; Pinna, F.; Strukul, G. *Catal. Today* **2005**, *104*, 323−328.
(26) Pashkova, A.; Svajda, K.; Dittmeyer, R. *Chem. Eng. J.* **2008**, *139*, 164−171.
(27) Pashkova, A.; Dittmeyer, R.; Kaltenborn, N.; Richter, H. *Chem. Eng. J.* **2010**, *165* (3), 924−933.
(28) Shi, L.; Goldbach, A.; Zeng, G.; Xu, H. *Catal. Toady* **2010**, *156*, 118−123.
(29) Wang, X.; Nie, Y.; Lee, J. L. C.; Jaenicke, S. *Appl. Catal., A* **2007**, *317*, 258−265.
(30) Ng, J. F.; Nie, Y.; Chuah, G. K.; Jaenicke, S. *J. Catal.* **2007**, *269*, 302−308.
(31) Voloshin, Y.; Lawal, A. *Appl. Catal., A* **2009**, *353*, 9−16.
(32) Voloshin, Y.; Halder, R.; Lawal, A. *Catal. Today* **2007**, *125*, 40−47.
(33) Volshin, Y.; Lawal, A. *Chem. Eng. Sci.* **2009**, *65*, 1028−1036.
(34) Inoue, T.; Schmidt, M. A.; Jensen, K. F. *Ind. Eng. Chem. Res.* **2007**, *46* (4), 1153−1160.
(35) Inoue, T.; Ohtaki, K.; Murakami, S.; Matsumoto, S. *Fuel Process. Technol.* **2012**, DOI: http://dx.doi.org/10.1016/j.fuproc.2012.04.009.
(36) Gemo, N.; Biasi, P.; Canu, P.; Salmi, T. O. *Chem. Eng. J.*, 2012, http://dx.doi.org/10.1016/j.cej.2012.07.015.
(37) Deguchi, T.; Yamano, H.; Iwamoto, M. *J. Catal.* **2012**, *287*, 55−61.
(38) Biasi, P.; Canu, P.; Menegazzo, F.; Pinna, F.; Salmi, T. O. *Ind. Eng. Chem. Res.* **2012**, *51*, 8883−8890.
(39) Biasi, P.; Menegazzo, F.; Pinna, F.; Eränen, K.; Salmi, T. O.; Canu, P. *Chem. Eng. J.* **2011**, *176−177*, 172−177.
(40) Kim, J.; Chung, Y.; Kang, S.; Choi, C.; Kim, B.; Kwon, Y.; Kim, T. J.; Oh, S.; Lee, C. *ACS Catal.* **2012**, *2* (6), 1042−1048.
(41) Sankar, M.; Morad, M.; Pritchard, J. C.; Freakley, S. J.; He, Q.; Edwards, J. K.; Taylor, S.; Carley, A. F.; Knight, D.; Kiely, C. J.; Hutchings, G. J. *ACS Nano* **2012**, *6* (8), 6600−6613.
(42) Van Herk, D.; Castaño, P.; Makkee, M.; Moulijn, J. A.; Kreutzer, M. T. *Appl. Catal., A* **2009**, *365*, 199−206.
(43) Marquez, N.; Castano, P.; Makkee, M.; Moulijn, J. A.; Kreutzer, M. T. *Chem. Eng. Technol.* **2008**, *31* (8), 1130−1139.
(44) Kreutzer, M. T.; Kapteijn, F.; Moulijn, J. A.; Heiszwolf, J. J. *Chem. Eng. Sci.* **2005**, *60* (22), 5895−5916.
(45) Samanta, C. *Appl. Catal., A* **2008**, *350*, 133−149.
(46) Descamps, C.; Coquelet, C.; Boualloum, C.; Richon, D. *Thermochim. Acta* **2005**, *430*, 1−7.
(47) Edwin, N. N.; Piccinini, M.; Pritchard, J. C.; Edwards, J. K.; Carley, A. F.; Moulijn, J. A.; Hutchings, G. J. *ChemSusChem* **2009**, *2*, 575−580.
(48) Piccinini, M.; Ntainjua, E. N.; Edwards, J. K.; Carley, A. F.; Moulijn, J. A.; Hutchings, G. J. *Phys. Chem. Chem. Phys.* **2010**, *12*, 2488−2492.
(49) Piccinini, M.; Edwards, J. K.; Moulijn, J. A.; Hutchings, G. J. *Catal. Sci. Technol.* **2012**, *2*, 1908−1913.